

# Formation and Long Term Evolution of an Externally Driven Magnetic Island in Rotating Plasmas<sup>\*</sup>)

Yasutomo ISHII and Andrei SMOLYAKOV<sup>1)</sup>

*Japan Atomic Energy Agency, Ibaraki 311-0102, Japan*

<sup>1)</sup>*University of Saskatchewan, Saskatoon SK S7N 5E2, Canada*

(Received 27 December 2007 / Accepted 29 May 2008)

Alfven resonance effects on the evolution of a magnetic island driven by an externally applied perturbation are investigated for rotating plasmas. The simulation results show the importance of Alfven resonance for obtaining a perturbed current profile and estimating a critical value of the external perturbation, beyond which the magnetic island grows rapidly. The nonlinear evolution of the externally driven magnetic island is also investigated at low and high viscosities  $\nu$ . It is shown that the transition phase accompanying the secondary reconnection at the initial X-point in the driven magnetic island evolution occurs in low resistivity and viscosity plasmas.

© 2008 The Japan Society of Plasma Science and Nuclear Fusion Research

Keywords: plasma rotation, magnetic island, secondary reconnection, Alfven resonance

DOI: 10.1585/pfr.3.048

## 1. Introduction

Several issues related to activities based on magneto-hydrodynamics (MHD) that must be resolved to achieve a high performance tokamak plasma. The neoclassical tearing mode (NTM), which severely affects the performance of a fusion reactor [1], is one such issue. Therefore, the suppression and control of the magnetic island is an important topic in tokamak fusion research. One mechanism of magnetic island formation is the unstable tearing modes driven by the gradient of the equilibrium current or a pressure gradient. Another important mechanism of the magnetic reconnection is the drive by externally applied perturbations, such as the residual error fields in the magnetic coils, or due to MHD activities. The latter process is considered to be a possible candidate for the formation of the seed island for NTM, where an MHD event such as the sawtooth oscillation acts as the external perturbation for the target mode through toroidal mode coupling.

In tokamak plasmas, plasma rotation is excited by external momentum inputs such as the neutral beam injection (NBI), or the self organization of the plasma flow by plasma turbulence. The plasma rotation affects the stability and evolution of MHD modes. Spontaneous and externally driven magnetic islands are also affected by the plasma rotation. In this study, we focus on the effects of plasma rotation on the externally driven magnetic island. An externally driven magnetic island can be suppressed by plasma rotation for an external perturbation amplitude lower than some threshold value, which has been extensively studied previously [2]. When the external perturbation becomes larger than a critical value, and the plasma

rotation becomes low around the magnetic neutral surface, where  $\mathbf{k} \cdot \mathbf{B} = 0$ , a driven magnetic island begins to grow rapidly. For rotation damping around the magnetic neutral surface, the perturbed current and magnetic field profiles are important. In rotating plasmas, the perturbed current is formed around the Alfven resonance surface [3–5]. The radial position of the Alfven resonance deviates from that of the magnetic neutral surface. Some theoretical studies [6, 7] show the steady state solution with and without the magnetic island, including the Alfven resonance effect. However, a dynamic process by which Alfven resonance current causes a driven magnetic island has not been studied. Hence, it is important to study the process by which the perturbed current sheet, which is formed at the Alfven resonance surface, drives the evolution of the magnetic island. The former theoretical studies are based on the asymptotic matching method, which divides the plasma region in two regions, the inner non-ideal and outer ideal region. Hence, these theoretical studies are applicable only for a magnetic island that is small compared to the inner layer width. Another important assumption is the steady state  $\partial/\partial t = 0$ . The importance of the non-steady state on the rapid onset condition of the externally driven magnetic island has been reported previously [8]. In this study, we investigate the Alfven resonance effects on the driven magnetic island formation in the rotating plasma.

In addition, the performance of a magnetically confined plasma depends on the long term behavior of a driven magnetic island. Some important features of the long term evolution of an externally driven magnetic island have been reported previously [8], such as the appearance of the transition phase, which becomes clearer and longer as the resistivity becomes low [8]. In this study, we investigate

author's e-mail: [ishii.yasutomo@jaea.go.jp](mailto:ishii.yasutomo@jaea.go.jp)

<sup>\*</sup>) This article is based on the invited talk at the 24th JSPF Annual Meeting (2007, Himeji).

the viscosity effects on the long term evolution of the externally driven magnetic island. As shown in a previous study [8], a critical external magnetic perturbation depends very weakly on the viscosity in the low regime  $\nu \leq 10^{-6}$ , whereas in the high viscosity regime  $\nu \geq 10^{-6}$ , a critical external magnetic perturbation depends on the viscosity. Hence, in this study, we use  $\nu = 10^{-7}$  as a typical low viscosity, and  $\nu = 10^{-4}$  as a typical high viscosity.

## 2. Basic Equations

To investigate the time evolution of a magnetic island caused by an externally applied magnetic flux perturbation in a rotating plasma, the resistive reduced magnetohydrodynamic (MHD) equations are used in the cylindrical geometry  $(r, \theta, \varphi = z/R_0)$ ,

$$\frac{\partial}{\partial t} \Psi = \frac{1}{r} [\Psi, \phi] + \frac{B_0}{R_0} \frac{\partial}{\partial \varphi} \phi + \eta J - E, \quad (1)$$

$$\frac{\partial}{\partial t} U = \frac{1}{r} [U, \phi] + \frac{1}{r} [\Psi, J] + \frac{B_0}{R_0} \frac{\partial J}{\partial \varphi} + \nu \nabla_{\perp}^2 (U - U_0), \quad (2)$$

$$J = \nabla_{\perp}^2 \Psi, \quad U = \nabla_{\perp}^2 \phi,$$

$$\mathbf{B} = B_0 \mathbf{e}_{\varphi} + \mathbf{e}_{\varphi} \times \nabla \Psi, \quad \mathbf{V} = \mathbf{e}_{\varphi} \times \nabla \phi.$$

Here,  $\Psi$  is the azimuthal (poloidal) magnetic flux function,  $\phi$  is the flow potential,  $J$  is the plasma current,  $U$  is the vorticity,  $B_0$  is the axial (toroidal) magnetic field at the magnetic axis, and  $2\pi R_0$  is the periodicity in the axial direction, where  $R_0/a$  corresponds to the aspect ratio of a tokamak, which is set to 10 in the following simulations. The safety factor  $q(r)$  in equilibrium is given by  $q^{\text{EQ}}(r) = rB_0/R_0(d\Psi^{\text{EQ}}(r)/dr)$ .  $\eta$  and  $\nu$  are the plasma resistivity and the viscosity, respectively.  $U_0$  is the vorticity corresponding to the plasma poloidal rotation and the last term in Eq. (2) is included to maintain the plasma rotation in the steady state. The operator  $\nabla_{\perp}$  expresses the differentiation in the  $(r, \theta)$  coordinate. Parameters in these equations are normalized by the plasma minor radius  $a$ , and the poloidal Alfvén time  $\tau_{\text{pa}} = \sqrt{\rho}a/B_{\theta}(a)$ , where the plasma mass density  $\rho$  has been set as 1. Then the resistivity  $\eta$  and viscosity  $\nu$  are normalized such that  $\eta = \tau_{\text{pa}}/\tau_{\eta}$  and  $\nu = \tau_{\text{pa}}/\tau_{\nu}$ , respectively, where  $\tau_{\eta}$  is the plasma skin time and  $\tau_{\nu}$  is the viscous diffusion time. The finite differential method is used to solve Eqs. (1) and (2), in the radial discretization, and Fourier decomposition is used in the poloidal and toroidal directions. This study uses up to 1600 radial grids and 20 harmonics. The time step is advanced by the predictor corrector time integration scheme with a typical time step of  $\Delta t = 5 \times 10^{-5}$ .

In the following, we consider a plasma with a  $q = 2$  resonant surface, which is stable against the tearing mode,  $\Delta' < 0$ , and we study the MHD modes with a single helicity of  $m/n = 2/1$  for simplicity, where  $(m, n)$  is the poloidal and toroidal mode numbers. In addition, we consider the rigid rotation of plasma in the following, which corresponds to the stream function of  $\phi_{0/0}(r) = (V_{\theta a}/2a)r^2$

and a vorticity of  $U_{0/0} = 2V_{\theta a}/a$ , where  $V_{\theta a}$  is the poloidal flow velocity at the wall. In the following, we set  $V_{\theta a} = 2\pi a/100$ , which correspond to the normalized plasma rotation frequency of  $10^{-2}$ . The external magnetic perturbation  $\Psi^{\text{ext}}$  is added at the plasma surface as a linearly increasing poloidal flux function,  $\Psi_{2/1}(r = a) = \Psi^{\text{ext}}(t) = (d\Psi^{\text{ext}}/dt) \cdot (t - t_0)$ . In this study,  $t_0$  is set as 10 numerically confirm that the state is stationary without an external perturbation. Here,  $(d\Psi^{\text{ext}}/dt)$  is the increasing rate of external perturbation.

## 3. Current Sheet Formed by the Alfvén Resonance

The magnetic island is usually formed by a current sheet at the resonant surface (magnetic neutral surface), where  $\mathbf{k} \cdot \mathbf{B} = 0$ . When background rotation does not exist, a current sheet caused by an externally applied perturbation is formed at the magnetic neutral surface. However, when background rotation exists, a current sheet forms at the both sides of the magnetic neutral surface. This difference of the radial positions between a current sheet and a magnetic neutral surface originates from the Alfvén resonance condition. The Alfvén resonance condition for the reduced MHD model is obtained from the linear ideal reduced MHD eqs..

$$\frac{\partial}{\partial t} \psi = B_0 \mathbf{e}_z \cdot \nabla \phi - v_{\theta 0} \cdot \nabla_{\perp} \psi, \quad (3)$$

$$\frac{\partial}{\partial t} \nabla_{\perp}^2 \psi + v_{\theta 0} \cdot \nabla \nabla_{\perp}^2 \phi = B_0 \mathbf{e}_z \cdot \nabla \nabla_{\perp}^2 \psi. \quad (4)$$

By assuming the form  $f = f \exp\{i(\mathbf{k} \cdot \mathbf{x} - \omega t)\}$  for  $\psi$  and  $\phi$ , the Alfvén resonance condition is obtained for  $\omega = 0$ .

$$(m\Omega_{\theta 0/0})^2 = (k_{\parallel} B_0)^2 \quad (5)$$

Hence, in the case of finite rotation  $v_{\theta 0} \neq 0$ , the Alfvén resonance condition is satisfied at both sides of the magnetic neutral surface,  $k_{\parallel} B_0 = 0$ . Figure 1 shows a radial profile of the perturbed current drawn along the line through the maximum of the perturbed current around the magnetic neutral surface, where the safety factor is  $q = 2$ , obtained numerically for  $\eta = 10^{-6}$  and  $\nu = 10^{-7}$ . As shown in Fig. 1, when the rotation frequency is sufficiently large, two positive peaks of perturbed current appear at both sides of the magnetic neutral surface, and the perturbed current becomes negative at the magnetic neutral surface. As the rotation frequency decreases, the radial position of the current peaks approaches the magnetic neutral surface. When the rotation frequency becomes sufficiently low, two positive peaks of the perturbed current merge into one. Figure 2 shows the 2D contour of the perturbed current in the radial and poloidal directions for  $\Omega_{\theta 0/0} = 2.0 \times 10^{-2} \pi$ ,  $\eta = 10^{-6}$  and  $\nu = 10^{-7}$ . As shown in Fig. 2, two pairs of the maximum and minimum of the perturbed current are formed in the poloidal direction, because the safety factor at the magnetic neutral surface is  $q = 2$ . The perturbed

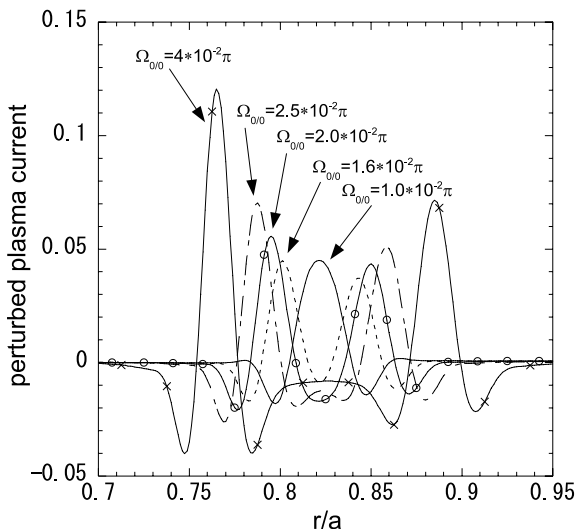


Fig. 1 Radial profile of the perturbed current formed around the magnetic neutral surface due to externally applied perturbation. The resistivity  $\eta$  is  $10^{-6}$  and the viscosity  $\nu$  is  $10^{-7}$ . As the rotation frequency becomes high, the distance between the magnetic neutral surface and the perturbed current peak becomes large.

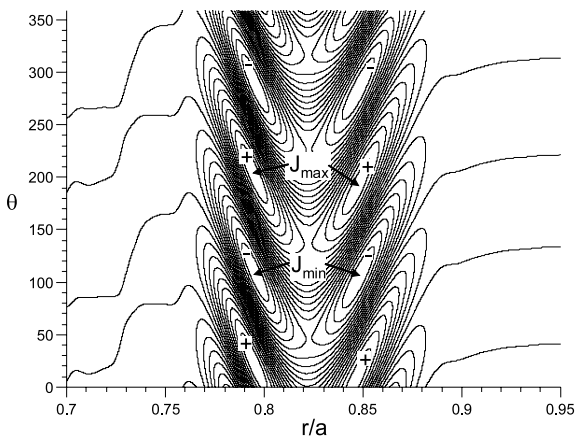


Fig. 2 Two-dimensional profile of the perturbed current obtained for the rotation frequency  $\Omega_{0/0} = 2.0^{-2}\pi$ , resistivity  $\eta = 10^{-6}$ , and viscosity  $\nu = 10^{-7}$ . Two sets of positive and negative current sheets appear in the poloidal direction.

current forms the current sheet, which crosses the magnetic neutral surface with an angle of less than 90 degrees. This is because of the finite background rotation. In the vicinity of the magnetic neutral surface, the perturbed current is very small. Figure 3 shows the time evolution of the radial position of the Alfvén resonance, which is estimated from Eq. (5), and the maximum and minimum of the perturbed current. As shown in Fig. 3, the radial position of the Alfvén resonance moves to the magnetic neutral surface. This is because the background flow is damped by the appearance of the magnetic island, which applies

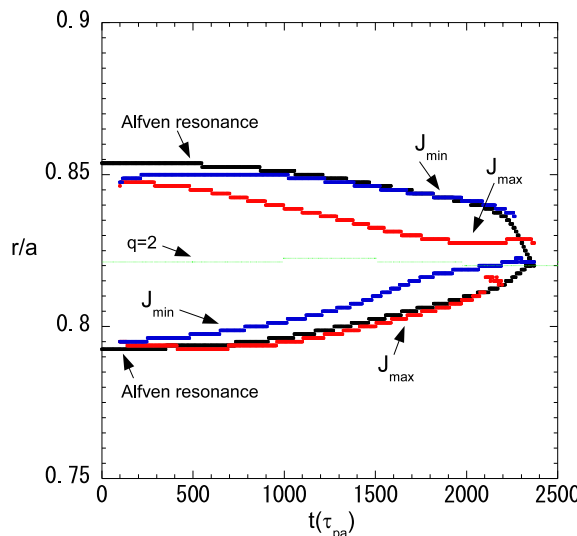


Fig. 3 Time evolution of the radial position of the Alfvén resonance and the maximum and minimum of the perturbed current for the rotation frequency  $\Omega_{0/0} = 2.0^{-2}\pi$ , resistivity  $\eta = 10^{-6}$ , and viscosity  $\nu = 10^{-7}$ . In the initial phase, the maximum and minimum peaks of the perturbed current move, following the Alfvén resonance surface.

torque on the plasma. As shown in Fig. 1, the peaks of the perturbed current approach the magnetic neutral surface as the rotation frequency becomes small. In the rotating plasma, the magnetic island driven by the externally applied perturbation grows slowly while the rotation frequency is sufficiently large. When the rotation frequency becomes lower than a critical value, the driven magnetic island grows rapidly [2]. Therefore, just before the rapid onset of the magnetic island, the radial position of the Alfvén resonance has almost the same position as the magnetic neutral surface. At this time, the two maximum and minimum peaks of the perturbed current become single peaks. This is the first result showing how the current sheet developed by Alfvén resonance triggers the rapid onset of the magnetic island.

In previous theoretical studies, the effects of Alfvén resonance are not considered, and the perturbed current is assumed to be localized at the magnetic neutral surface. Hence, the plasma region is divided into an external ideal and inner non-ideal one. The distance between the radial position of the Alfvén resonance current sheet and magnetic neutral surface depends on the magnetic shear and the rotation frequency. In a low collisionality plasma, there is a possibility that the width of the inner non-ideal region is small compared with this distance, as shown in this section. Therefore, in such a case, the Alfvén resonance current sheet exists in the external ideal region. This suggests that a new analytical theory that includes the effects of the Alfvén resonance current sheet is required to derive the analytical formula of the driven magnetic island evolution in a rotating plasma in the flow-suppressed growth phase.

## 4. Viscosity Effects on the Rotation Damping

Plasma rotation is damped by the torque applied by an external perturbation. The total torque consists of the electromagnetic, inertial, and viscous torque. In previous theoretical and numerical works [2, 9], the high viscosity regime, which corresponds to the visco-resistive regime, is mainly discussed. In a high temperature plasma, however, the viscosity and resistivity become low, because of the low collisionality. In this section, we investigate the viscosity effects on the evolution of a driven magnetic island. Figures 4(a) and (b) show the radial profile of the total torque for low viscosity,  $\nu = 10^{-7}$ , and high viscosity,  $\nu = 10^{-4}$ . In both cases, the resistivity is  $\eta = 10^{-6}$  and the rotation frequency is  $\Omega_{0/0} = 2 \times 10^{-2}\pi$ . For low viscosity, the viscous torque is small compared with the electromagnetic and inertial torques. When the viscosity is high, during the flow-suppressed phase, the inertial torque is small compared with the electromagnetic and the viscous torques. This result is consistent with the previous theoretical assumption. Although the main components of the total torque differ between the low and high viscosity cases, the total torque localizes around the magnetic neutral surface and Alfvén resonance surfaces, as shown in Fig. 4. This torque localization around the magnetic neutral and Alfvén resonant surfaces is consistent with the current sheet profile shown in Fig. 2, which localizes around the Alfvén resonance surfaces. One important feature of the torque profile is that the torque expands to a region wider than the width of the magnetic island, which is formed at the magnetic neutral surface, as shown in Fig. 4. In the former theory, the asymptotic matching procedure is used to connect the outer ideal and inner non-ideal regions, and the torque is assumed to be exerted on the inner region. By

considering the Alfvén resonance current sheet, the region where the torque acts differs from the former theoretical treatment.

Figures 5(a) and (b) show the time evolution of the background plasma rotation,  $v_{\theta 0/0}$ , for (a)  $\nu = 10^{-7}$  and (b)  $\nu = 10^{-4}$ . In both cases, the resistivity is set as  $\eta = 10^{-6}$ . In the low viscosity case, as shown in Fig. 5(a), the background rotation is damped in the narrow radial region localized around the Alfvén resonance surfaces. This is consistent with the torque profile shown in Fig. 4(a). During the initial phase of  $0 \leq t \leq 1800$ , the background rotation is damped strongly at both sides of the magnetic neutral surface, which corresponds to two peaks of the perturbed current. As the rotation becomes small at the magnetic neutral surface, the radial position of the Alfvén resonance and perturbed current peaks approach the magnetic neutral surface. Therefore, the background rotation is damped strongly at the magnetic neutral surface after  $t \approx 2000$ . On the other hand, when the viscosity is high, as shown in Fig. 5(b), the background rotation is damped in the wide radial region, which extends almost over the entire plasma region. This aspect of background rotation damping is not in accord with the torque profile localized in the narrow region shown in Fig. 4(b). In order to understand this difference between background rotation damping and the torque profile in the high viscosity regime, a numerical simulation, in which the viscosity is set as zero for  $m/n = 0/0$ -harmonics and  $\nu = 10^{-4}$  except for  $m/n = 0/0$ -harmonics, was executed. Figure 6 shows the time evolution of the background rotation profile, excluding the viscosity effects on the  $m/n = 0/0$ -harmonics. In this case, the background flow is damped in the narrow region compared with the case that includes the viscosity effects on  $m/n = 0/0$ -harmonics. This means that the background flow damping

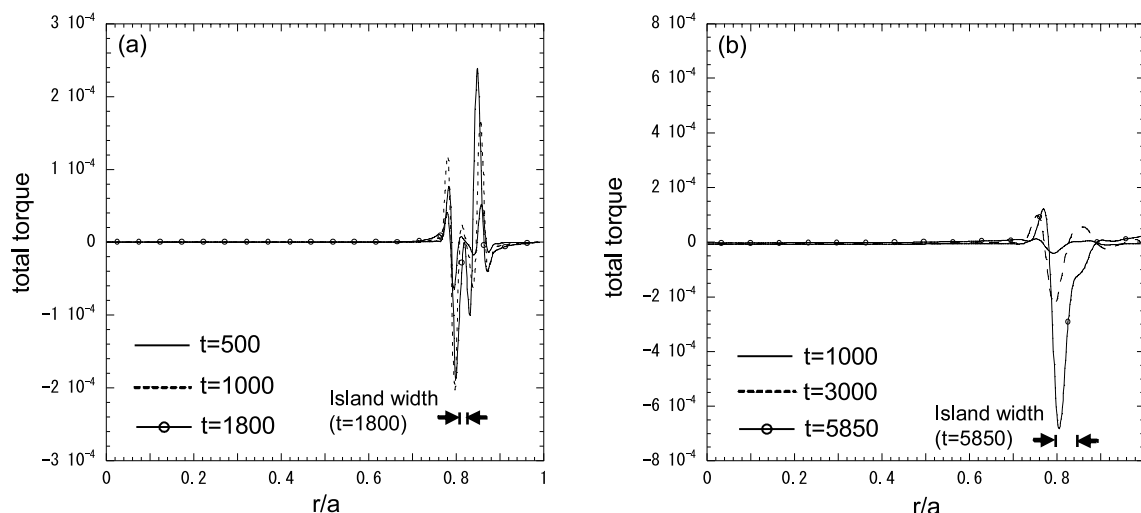


Fig. 4 Time evolution of the total torque for (a)  $\nu = 10^{-7}$  and (b)  $\nu = 10^{-4}$ . In both cases, the initial rotation frequency is  $\Omega_{0/0} = 2.0 \cdot 10^{-2}\pi$  and the resistivity is  $\eta = 10^{-6}$ . In both cases, the total torque localizes around the Alfvén resonance surfaces, but expands wider than the magnetic island width.

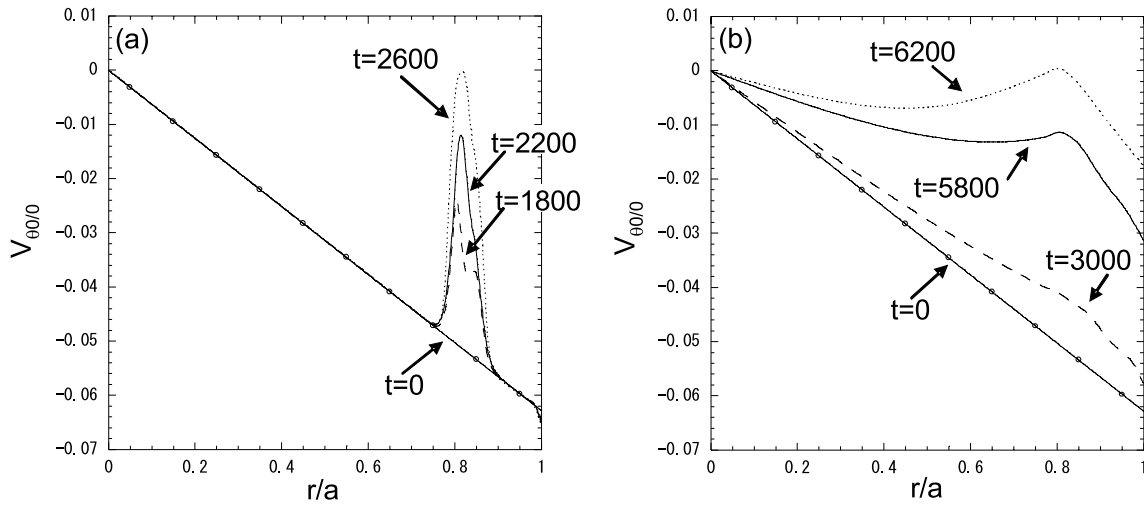


Fig. 5 Time evolution of the background rotation for (a)  $\nu = 10^{-7}$  and (b)  $\nu = 10^{-4}$ . In both cases, the initial rotation frequency is  $\Omega_{0/0} = 2.0^{-2}\pi$  and the resistivity is  $\eta = 10^{-6}$ . In the low viscosity case, the background rotation is damped in the localized region around the Alfvén resonance. In the high viscosity regime, however, the background rotation is damped over almost the entire plasma region.

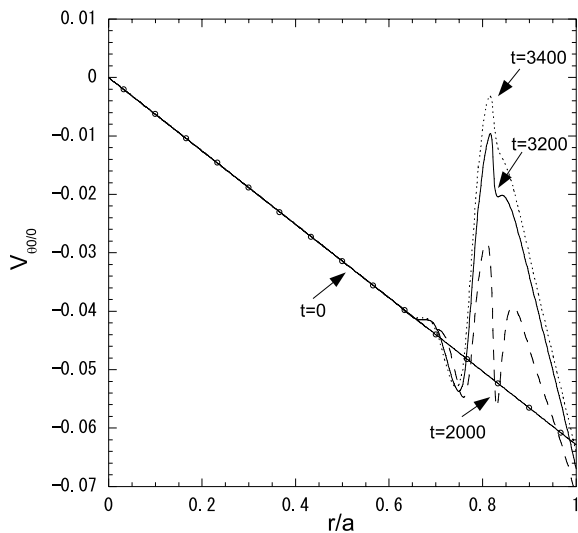


Fig. 6 Time evolution of the background rotation for the case without the viscosity effects on  $m/n = 0/0$ -harmonics. For higher harmonics, the viscosity is  $\nu = 10^{-4}$ . The initial rotation frequency is  $\Omega_{0/0} = 2.0^{-2}\pi$  and the resistivity is  $\eta = 10^{-6}$ . In this case, the background rotation is damped in a more narrow region than when including the viscosity effects on the  $m/n = 0/0$ -mode.

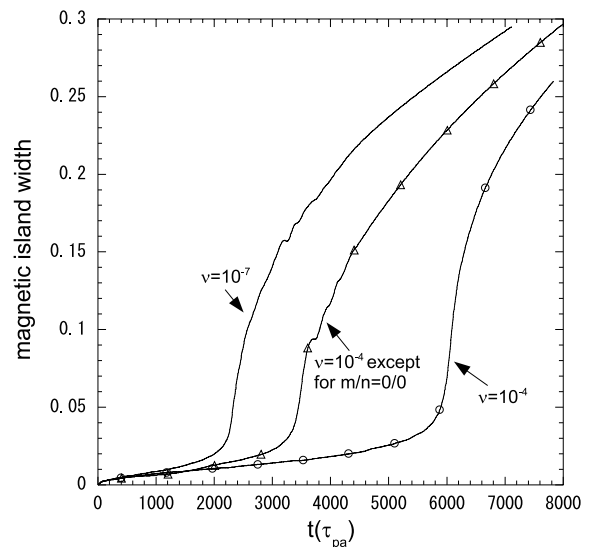


Fig. 7 Time evolution of the magnetic island width for  $\nu = 10^{-7}$ ,  $\nu = 10^{-4}$  and  $\nu = 10^{-4}$  except for the  $m/n = 0/0$  harmonics. The initial rotation frequency is  $\Omega_{0/0} = 2.0^{-2}\pi$  and the resistivity is  $\eta = 10^{-6}$ . The trigger timing of the rapid growth of the driven magnetic island becomes faster by excluding the viscosity effects on the  $m/n = 0/0$ -mode.

in the entire plasma region obtained for the high viscosity regime originated from the viscosity effect on  $m/n = 0/0$ -harmonics. Even in the case excluding the viscosity effect on  $m/n = 0/0$ -harmonics, the background rotation is damped. This is caused by the quasi-linear effects from the higher harmonics on  $m/n = 0/0$ -one. In both cases shown in Figs. 5 (b) and 6, the external perturbation is increased by the same rate at the plasma edge. Hence, the

input rates of the magnetic flux into the system are the same. However, the background rotation becomes zero at  $t \sim 6200$  when the viscosity effects on all harmonics are considered, and at  $t \sim 3400$  when the viscosity effects on  $m/n = 0/0$ -harmonics are not considered. Figure 7 shows the time evolution of the magnetic island width driven by an externally applied perturbation for different viscosities, where the resistivity is set to  $\eta = 10^{-6}$ . In the high viscosity regime, the torque is localized in the narrow radial

region, but the background flow is damped over the wide radial region because of the viscosity effect on  $m/n = 0/0$ -harmonics. The trigger timing of the onset of the rapid growth of the magnetic island is delayed by increasing the viscosity, as shown in Fig. 7.

## 5. Nonlinear Evolution of the Driven Magnetic Island

In this section, some viscosity effects on the nonlinear evolution of the driven magnetic island are shown. Some

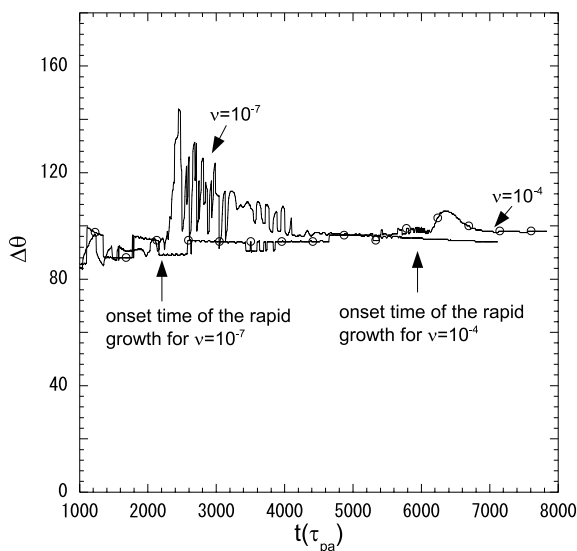


Fig. 8 Time evolution of the phase difference between the O-point and the X-point in the poloidal angle for  $\nu = 10^{-7}$  and  $\nu = 10^{-4}$ . In both cases,  $\Omega_{0/0} = 2.0^{-2}\pi$  and the resistivity is  $\eta = 10^{-6}$ . The phase difference  $\Delta\theta$  becomes larger for low viscosity compared with high viscosity.

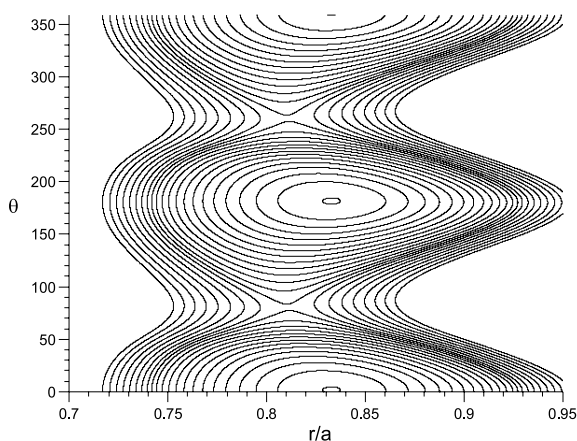


Fig. 9 Contour plot of the helical flux function, i.e. magnetic island, at  $t = 6600$  for the rotation frequency  $\Omega_{0/0} = 2.0^{-2}\pi$ , the resistivity  $\eta = 10^{-6}$  and the viscosity  $\nu = 10^{-4}$ . Even when  $\Delta\theta$  becomes maximum, the secondary island is not formed at the initial X-point.

resistivity effects on the nonlinear evolution of the driven magnetic island has been reported previously [8]. For a low viscosity case,  $\nu = 10^{-7}$ , the magnetic island width appears to oscillate after the rapid growth phase, as shown in Fig. 7. In this transition phase, a secondary reconnection occurs at the initial X-point due to the deformation of the magnetic island in the poloidal direction. The degree of this deformation in the poloidal direction can be estimated by the phase difference between the X- and O-points. Figure 8 shows the time evolution of the phase difference between the X- and O-points in the poloidal direction. In both cases, the resistivity is set as  $\eta = 10^{-6}$ . For low viscosity, the phase difference  $\Delta\theta$  changes from  $\Delta\theta \approx 90$  to  $\Delta\theta \approx 140$  during the rapid growth phase. After the rapid growth phase, the phase difference  $\Delta\theta$  oscillates from  $t \approx 2400$  to  $t \approx 4400$ . This duration corresponds to the transition phase, where the secondary reconnection occurs at the initial X-point [8]. For high viscosity, however, the phase difference  $\Delta\theta$  changes from  $\Delta\theta \approx 90$  to  $\Delta\theta \approx 105$  during the rapid growth phase. After the rapid growth phase, the phase difference  $\Delta\theta$  does not oscillate, but decreases monotonically from  $t \approx 6400$  to  $t \approx 6800$ . Figure 9 shows the contour plot of the magnetic island at  $t = 6600$  obtained for a high viscosity,  $\nu = 10^{-4}$ , and low resistivity,  $\eta = 10^{-6}$ . In the high viscosity case, the original X-point is clean-cut and the secondary magnetic island is not visible.

## 6. Summary

The Alfvén resonance effects on magnetic island evolution driven by an externally applied perturbation were investigated. In a low viscosity regime, a perturbed current sheet forms at the Alfvén resonance surfaces, which differ from the radial position of the magnetic neutral surface. In this case, a perturbed current sheet exists outside the inner non-ideal layer, defined for a non-rotating plasma. According to this perturbed current sheet profile, the total torque, which affects the plasma, extends wider than the radial position of the Alfvén resonance. These features are inconsistent with former theoretical assumptions, which enable using the asymptotic matching method to estimate the force balance and the critical value of the external perturbation, beyond which the driven magnetic island grows rapidly. Simulation results obtained in this study show the importance of taking into account the current sheet driven by the Alfvén resonance in estimating a critical value of external perturbation.

The nonlinear evolution of a driven magnetic island is also investigated in the wide parameter regime of the viscosity  $\nu$ . It is shown that in a high viscosity regime, background rotation is damped over almost the entire plasma region by the viscosity effect on the  $m/n = 0/0$ -harmonics. In the low viscosity regime, however, the background rotation is damped in a narrow region around the magnetic neutral surface and the Alfvén resonance surfaces. In the

high viscosity regime, it takes longer to damp the background rotation at the magnetic neutral surface compared with the low viscosity regime, because the torque acts to dampen the background rotation in the entire plasma region. When the background rotation becomes lower than a critical value, the driven magnetic island grows rapidly. In a low resistivity and viscosity regime, the driven magnetic island enters a transition phase, during which a secondary reconnection occurs at the initial X-point. In a high viscosity regime, however, the transition phase and the secondary reconnection are not observed in this study. Hence, the transition phase and secondary reconnection in the driven magnetic island evolution are distinctive features of a low resistivity and viscosity plasma.

In this study, we focused on the magnetic island formation and evolution driven by an external perturbation, increasing monotonously over time. An external perturbation becomes non-monotonous over time, if an MHD event

is considered as an origin. In such a case, the total torque exerted by an external perturbation [10] on an ideal or very low dissipative plasma becomes important from the viewpoint of the appearance and disappearance of the hysteresis of an externally driven magnetic island. This subject will be investigated in future studies.

- [1] A. Isayama *et al.*, Nucl. Fusion **43**, 1272 (2003).
- [2] R. Fitzpatrick, Phys. Plasmas **5**, 3325 (1998).
- [3] A. Hasegawa and L. Chen, Phys. Rev. Lett. **32**, 454 (1974).
- [4] X. Wang *et al.*, Phys. Plasmas **5**, 2291 (1998).
- [5] Z.W. Ma *et al.*, Phys. Fluids **3**, 2427 (1996).
- [6] O.A. Hurricane *et al.*, Phys. Plasmas **2**, 1976 (1995).
- [7] A. Boozer, Phys. Plasmas **3**, 4620 (1996).
- [8] Y. Ishii *et al.*, Nucl. Fusion **47**, 1024 (2007).
- [9] R. Fitzpatrick, Phys. Plasmas **10**, 1782 (2003).
- [10] J.B. Taylor, Phys. Rev. Lett. **91**, 115002 (2003).